STRENGTH
AND PLASTICITY

Structure and Impact Strength of Weld Joints Manufactured from a Pipe Steel with the Use of Hybrid Laser-Arc Welding

N. A. Tereshchenko[a], *, I. L. Yakovleva[a], M. A. Fedorov[b], A. B. Gizatullin[b], and T. S. Esiev[c]

[a] Institute of Metal Physics, Ural Branch, Russian Academy of Sciences, Ekaterinburg, 620108 Russia
[b] Chelyabinsk Pipe Rolling Plant, Chelyabinsk, 454129 Russia
[c] Gazprom VNIIGAZ, Razvilka, Leninskii okrug, Moscow oblast, 142717 Russia
*e-mail: tereshchenko@imp.uran.ru

Abstract—The weld joints of pipes with a diameter of 1420 mm and a pipe-wall thickness of 30 mm manufactured by two different technologies have been studied. These technologies were (i) combining the laser arc welding when making a root weld with the subsequent submerged arc welding when applying cap welds and (ii) the method of double-sided submerged arc welding. It has been shown that the first technology leads to the formation of a bainite-based disperse structure in weld joints, thereby providing a tough-ductile character of fracture and an increased level of impact strength for different positions of a notch with respect to the center of a weld joint.

INTRODUCTION

At the present time, the main pipelines for the transportation of oil and gas are manufactured from low-carbon low-alloy steels. The advanced technologies for the production of rolled sheets, including thermomechanical controlled processing and accelerated cooling, make it possible to obtain pipe steels of different strength level, among which the steels of strength grade K60 are the most demanded ones in the pipe production industry. The practice of their production shows that the application of contemporary equipment reliably ensures a complex of standard parameters regulated by the requirements to the chemical composition, weldability, and mechanical properties of pipe steels [1−3].

At a large volume of transported energy resources, an increase in the throughput capacity of a pipeline is attained by elevating the pressure of a transported reagent and the diameter of a pipe. The technological cycle of the manufacturing of large-diameter pipes includes the operation of welding. The method of submerged arc consumable electrode welding, which is widely applied for the production of such articles, implies the manufacturing of multipass joints and is accompanied by a high heat input to the welding bath, when an extensive heat input affected zone with a nonuniform microstructure and an increased level of microdistortions is formed near a weld joint [1, 4, 5].

The promising method of hybrid laser-arc welding (HLAW) provides the welding of rolled sheets with large thicknesses at a low heat input [6, 7]. Hybrid laser-arc welding is performed with the simultaneous use of two energy sources, such as a laser beam and an electrical arc, when the laser beam evaporates the metal appearing from metallic plasma and the flare stabilizes the arc discharge to result in the formation of a weld joint with deep metal welding [8−10]. The application of HLAW technology for the production of large-diameter pipes is reasonable from economic viewpoints, as HLAW differs from traditional submerged arc consumable electrode welding (SAW) by an increased rate [7, 9].

The physicometallurgical aspect of HLAW application is associated with the risk of the appearance of quenching-induced (quenched-in) structures and local embrittlement in the metal located in the heat-affected zone (HAZ) of a weld joint due to high cooling rates used in this method of welding [8, 11, 12]. The use of hybrid laser-arc welding in combination with the further manufacturing of cap welds by the method of submerged arc consumable electrode welding promotes the formation of a predominantly bainite structure in the metal of the near-weld zone and provides a higher brittle fracture resistance [13]. The welding of cap joints after the welding of a root joint is performed at minimum energy input rates, which provides the possibility to minimize the volume of heat-

Table 1. Chemical composition of steel, wt %

No.	C	Mn	Si	Cr	Ni	Cu	V	Mo	Ti	Nb
1	0.096	1.68	0.26	0.033	0.065	0.043	0.003	0.148	0.015	0.053
2	0.092	1.68	0.26	0.034	0.065	0.043	0.003	0.147	0.014	0.052

Table 2. Mechanical properties of steels after thermomechanical controlled processing

No.	σ_u, MPa	$\sigma_{0.2}$, MPa	δ, %	δ_{eqv}, %	ψ, %	$\sigma_{0.2}/\sigma_u$	KCV^{-60}, J/cm²	KCV^{-20}, J/cm²	HV_{10}, HV
1	610	530	23	11.4	35	0.87	333	339	211
2	620	540	24	10.5	35	0.87	378	338	211

affected zone in contrast to classic double-sided submerged multiarc welding. However, the industrial introduction of combined HLAW + SAW technology necessitates the stability and reproducibility of values for the impact strength as the most important characteristic for the structural durability of a weld joint and an article as a whole. This study is aimed at the solution of this problem and, for this purpose, it is necessary to investigate the crack propagation trajectory in a weld joint manufactured by the HLAW method under impact loading and to reveal the mechanisms of metal fracture in its individual zones.

EXPERIMENTAL

The material for study was the weld joints of tubes with a diameter of 1420 mm and a wall thickness of 30 mm. Welding was performed under workshop conditions by two different technologies. For the first group of weld joints, we used the combined technology, when the root joint was manufactured by HLAW in a medium of protective gases with the use of a consumed electrode, and the inner and outer joints were manufactured by automatic SAW. The second group of weld joints was manufactured by the conventional technology of double-sided automatic SAW.

The weld joints formed by different welding technologies were manufactured of individual single-melt sheets of a low-carbon low-alloy steel after thermomechanical controlled processing. The chemical composition of steel in the sheets (Table 1) is almost the same and corresponds to the requirements of GOST ISO 3183−2015 [14].

The identity of the chemical composition of steel provides the same weldability parameters $C_{equiv} = 0.42$ and $P_{cm} = 0.20$ and close values of mechanical characteristics (Table 2), which satisfy the conditions of normative documentation STO Gazprom 2-4.1-713-2013 [15].

The impact strength of weld joints was determined on Charpy V-notch specimens of type IX. Individual specimens differ from each other by the orientation of their mechanical notch with respect to the center of a

weld joint: it was placed in the center of a weld joint along the welding line. The tests were performed on an impact pendulum-type testing machine of series PSW and RKP-450.T at a temperature of −40°C. The cooling of specimens was carried out in a LOIP FT-311-80 thermostating laboratory device. The conditions of tests corresponded to GOST 6996−66 [16].

The macrostructure of weld joints was studied on polished metallographic specimens after etching in a 4-% nitric acid solution in ethanol on a NEOPHOT-30 optical microscope. The microstructure and fractures of weld-joint specimens after tests were studied on a Thermo Fisher Scientific scanning electron microscope. The data obtained in the course of fractographic study were compared with the metallographic data taken from the edge surface of an impact specimen fragment after impact loading.

The hardness was measured by the Vickers method at a load of 10 kgf.

RESULTS AND DISCUSSION

Structure of the Metal of Weld Joints

The macrostructure of weld joints is shown in Fig. 1. After etching, the surface of a metallographic polished specimen incorporates individual areas that differ from each other by the character of contrast. The basic metal has a poorly pronounced strip structure typical of pipe steels after thermomechanical controlled processing. The basis of this structure is a ferrite−bainite mixture with a small amount of degenerate perlite, and the average size of a ferrite grain is 2−4 μm. The hardness of such a structure is 211 HV. The weld joint manufactured by the hybrid technology contains a HLAW root joint and cap SAW joints, and each joint is surrounded by its heat-affected zone followed by the basic metal (Fig. 1a).

In the process of HLAW, heat impact takes place on a small surface area; the HLAW joint width is varied from 1.8 mm near the inner cap joint to 2.0 mm at the outer SAW joint (Fig. 1a, region *1*). In the process of melted metal crystallization, a zone of columnar
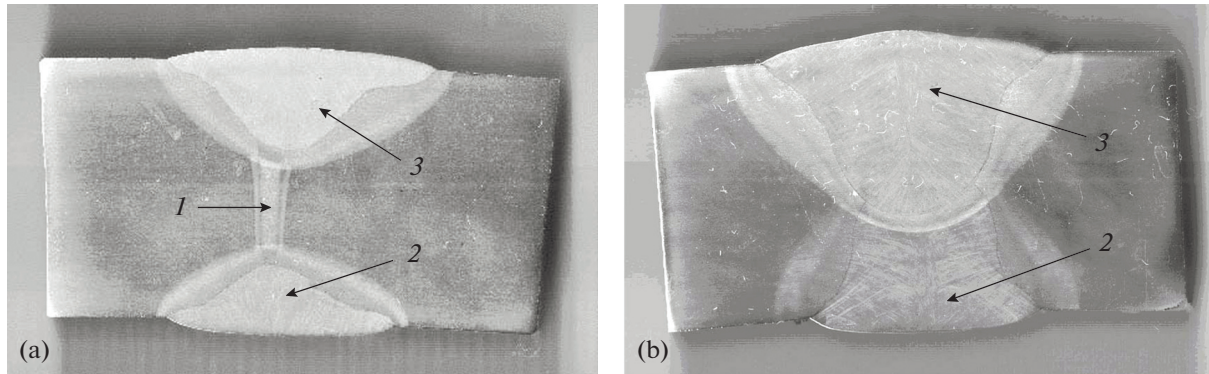
Fig. 1. Macrostructure in the cross sections of the weld joints manufactured by (a) hybrid and (b) conventional technologies: (*1*) HLAW joint, (*2*) inner cap SAW joint, (*3*) outer cap SAW joint.
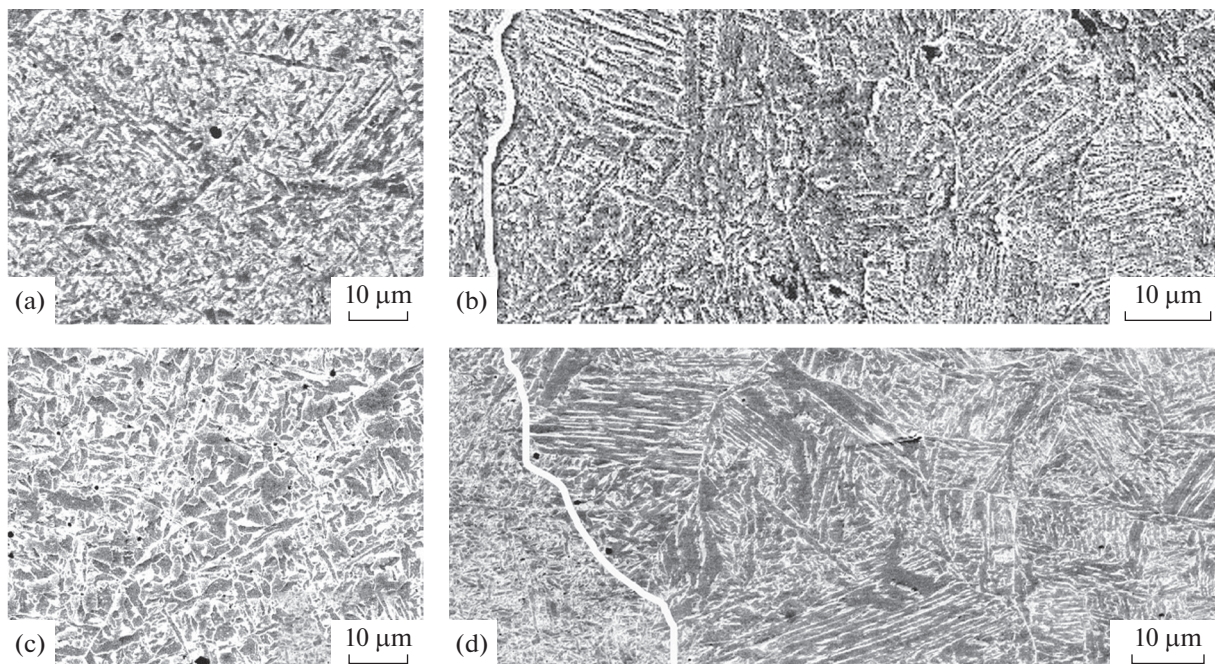

Fig. 2. SEM image of the structure of local zones in the weld joint manufactured by the hybrid technology: (a) root HLAW joint, (b) heat-affected zone of the HLAW joint in the overheating region, (c) outer cap SAW joint, (d) heat-affected zone of the outer cap SAW joint in the overheating region.

grains oriented from the welding line to the weld joint center with a width of 40–60 μm has been formed. The boundaries of grains are outlines with a ferrite framework, and extremely disperse α-bainite crystals have been formed in the body of grains (Fig. 2a). The melted metal of the weld joint is bounded with the welding line, behind which there is the heat-affected zone of the HLAW joint with a gradient structure with a length of from 0.5 to 1.0 mm. An overheating zone with a coarse-grained structure has been formed at temperatures close to the melting point (Fig. 2b). The size of a former austenite grain in the overheating zone is comparable with the width of columnar grains in the weld joint metal and attains 40–60 μm, and a bainite

structure of lath morphology predominates inside the grains. The average hardness of the weld joint metal and heat-affected zone is 257 HV and 274 HV, respectively. Such a level of hardness is formed as a result of phase recrystallization under cooling after HLAW heating and also under the influence of tempering processes during the manufacturing of cap SAW joints.

Due to the specifics of SAW thermal cycles [5], cap weld joints are much larger than an HLAW joint in their surface area (Fig. 1a, regions *2* and *3*). The width of the outer cap weld joint grows from 4–5 mm at the top to 30 mm near the surface. The average hardness of the metal of an SAW joint is 232 HV, being 10% lower than for an HLAW joint. The weld joint metal

Table 3. Impact strength of weld joint specimens

Welding technology	Notch orientation	KCV^{-40}, J/cm^2
Hybrid HLAW + SAW	Along the HLAW joint	315
	Along the welding line of the HLAW joint	311
Conventional SAW	At the center of the outer SAW joint	144
	Along the welding line of the outer SAW joint	56

structure is shown in Fig. 2c. The columnar structures of the metal of SAW and HLAW joints are similar, but their scales are different. The width of columnar crystals in the SAW joint attains 80−100 μm, being twice larger than for the HLAW joint. The α-bainite phase crystals in the body of a grain are much coarser. The heat-affected zone reproduces the SAW joint shape, and its width is varied from 2 to 8 mm in some regions due to a high heat input and low cooling rates after welding heating. The average size of a former austenite grain in the overheating zone is 100−120 μm, and the morphology of austenite decomposition products is characterized by broad diversity and incorporates lath and globular bainite crystals in equal proportions (Fig. 2d). The hardness of metal in the heat-affected zone of an SAW joint is ranged within 231−247 HV.

The weld joint manufactured by the conventional technology contains remelted metal in the inner and outer SAW joints (Fig. 1b). The states of metal in the SAW joints and the zone of their heat input are qualitatively similar, and the size of a "former" austenite grain near the welding line of the outer cap joint attains 150−200 μm, and the hardness is 224 HV.

Impact Strength and Fractography

The results of impact tests on the specimens of weld joints manufactured by the hybrid and classic technologies of welding (Table 3) indicate that all of them correspond to the established requirements to the values of KCV^{-40} to be 50 J/cm^2 [15]. In connection with the fact that the structure of weld joints is extremely non-uniform, the impact strength depends to an essential extent on the mutual arrangement of a weld joint and a notch in a specimen in all the methods of welding. However, on the whole, the data of this table indicate that the metal in the HLAW joint and near it demonstrates a much higher level of tis characteristic as compared to the SAW joint metal. Such a difference between the values of impact strength is produced by some specific features in the development of fracture in individual regions of weld joints.

The specimens containing an HLAW joint are characterized by the highest impact strength $KCV^{-40} = 315-311$ J/cm^2. The process of their fracture is energy consuming throughout the entire trajectory of the main crack.

In the specimen with a notch in the HLAW joint metal, the fracture surface formed under the notch
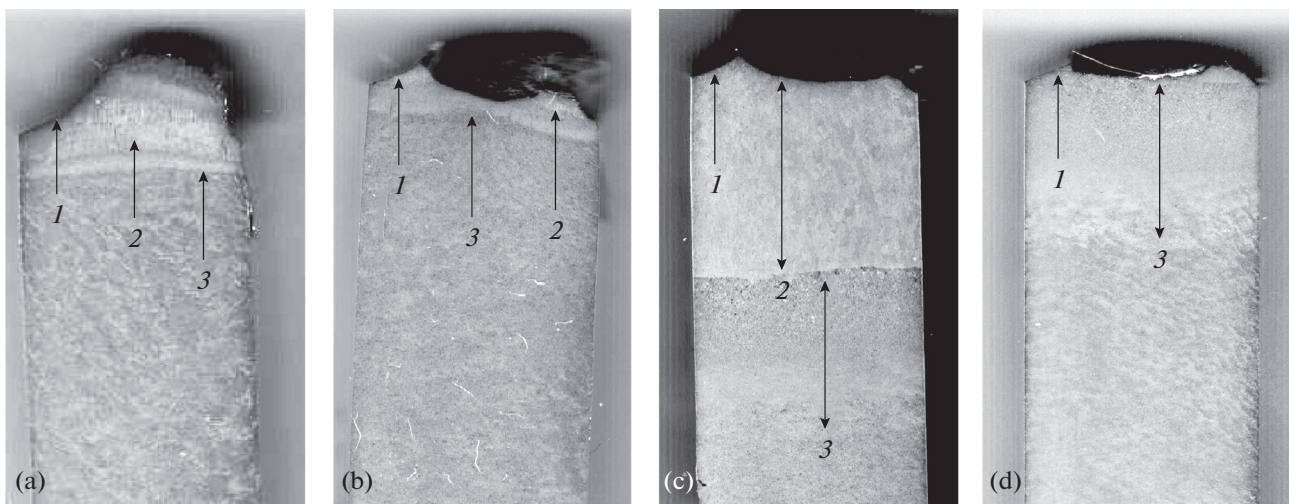

Fig. 3. Microstructure of weld joint specimen fragments after impact tests: (a), (b) hybrid welding technology with a notch (a) on the HLAW joint metal and (b) along the welding line of the HLAW joint and (c), (d) conventional welding technology with a notch (c) on the SAW joint metal and (d) along the welding line of the SAW joint: (*1*) notch, (*2*) weld joint metal, (*3*) hea-affected zone of a weld joint.
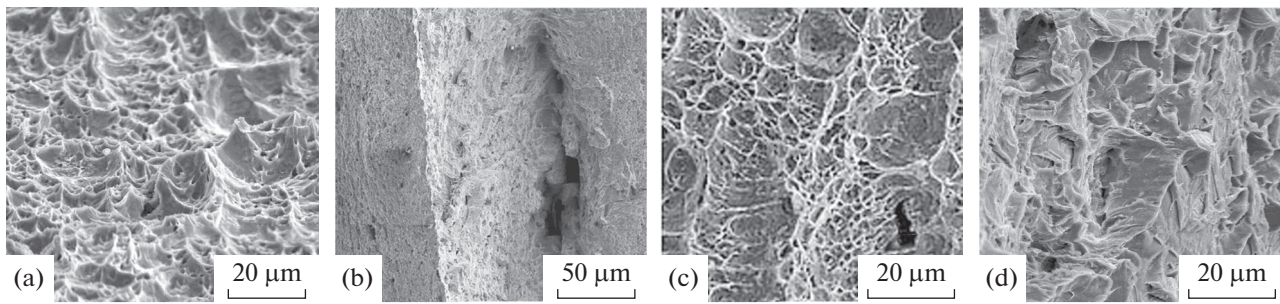
Fig. 4. Fractograms of a weld joint specimen with a notch on an HLAW joint: (a) crack nucleation region, (b–d) crack propagation region.
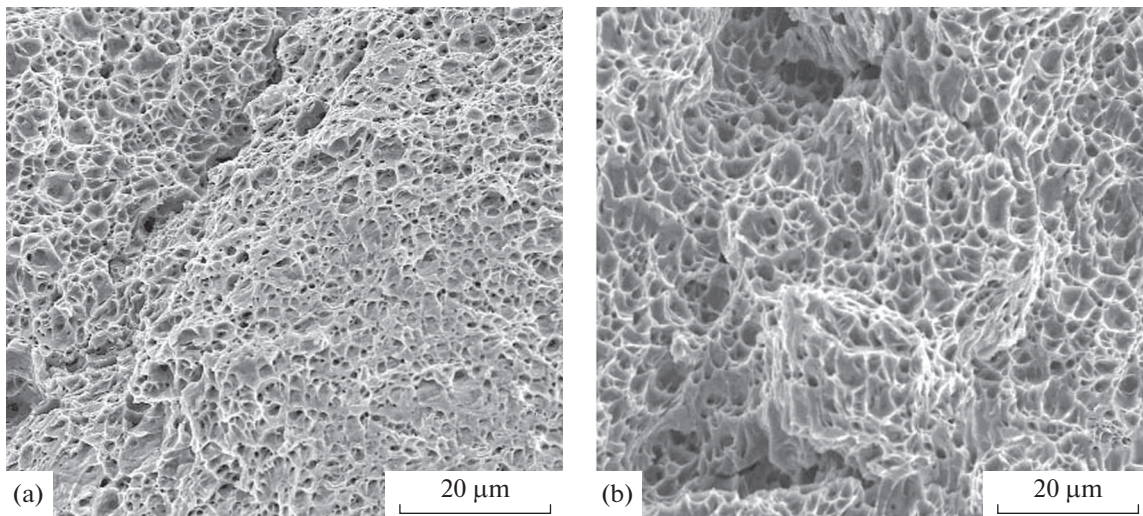

Fig. 5. Fractograms of a weld joint specimen with a notch along the welding line of an HLAW joint: (a) crack nucleation region, (b) crack propagation region.

during the nucleation of the main crack is no less than 20% of the fracture surface area and comes outside the weld joint metal to intersect the welding line and heat-affected zone of the weld joint (Fig. 3a).

In the fractograms taken in this fracture region, there are large dimples appearing by the mechanism of tough-ductile fracture via the formation and coalescence of micropores (Fig. 4a). The central fracture region formed at the main crack propagation stage passes through the basic metal of the weld joint (Fig. 3a). The fracture surface relief incorporates several "delamination cracks" with straightline flanges of tear (Fig. 4b). The surfaces oriented along the impact direction contain dimples grouped into rows parallel to tear flanges (Fig. 4c). They alternate with the quasi-brittle fracture areas elongated perpendicularly to the impact direction (Fig. 4d). The process of fracture is extremely energy consuming due to the formation of an extensive zone of the tough-ductile region of nucleation of a crack and the absorption of energy on the side edges of delamination cracks [17].

In the specimen with a notch along the welding line of the HLAW joint, the nucleation region of the main crack is less than 0.5 mm in width, and its surface is formed by planar small cups with rare quasi-chip facets (Fig. 5a). At the stage of development, the crack repeatedly changes the vector of its propagation to displace in the heat-affected zone at the moment of fracture, pass through the weld joint metal near the welding line, and returns to the heat-affected zone and further to the basic metal (Fig. 3b). The crack propagation region is presented by a hillocky surface of dimple fracture with abundance of secondary cracks (Fig. 5b). A high value of impact strength for this specimen is caused by a combination of two factors. In addition to the tough-ductile mechanism of steel fracture over the body of a grain, the fracture energy consumption is also influenced by "the effect of a composite specimen," when some regions of a weld joint divide the cross section of a specimen into "layers" of variable thickness with different structures, change the stressed
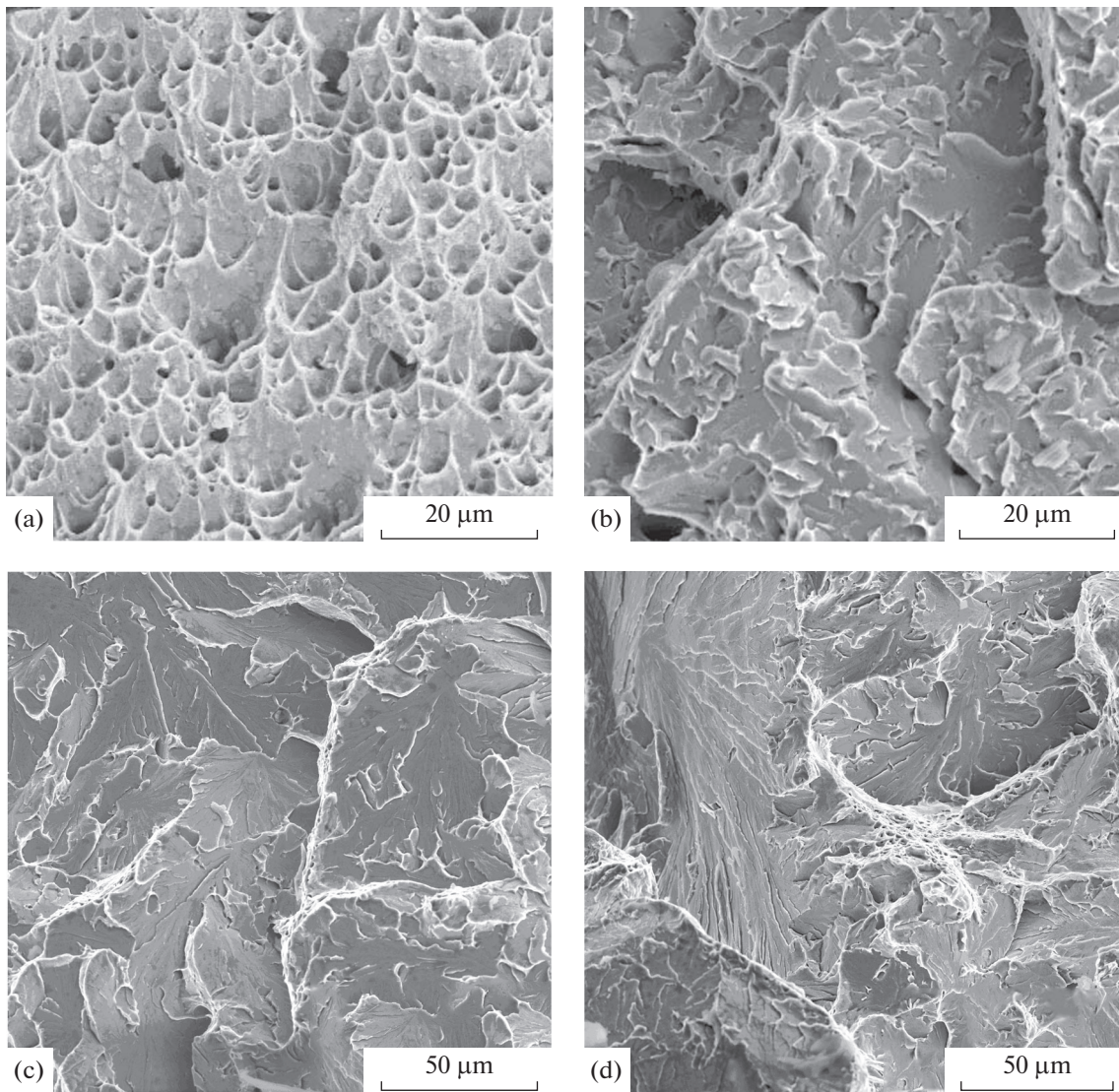
Fig. 6. Fractograms of fractures in weld joint specimens with a notch (a), (b) on the weld joint metal and (c), (d) along the welding line of an SAW joint: (a), (c) crack nucleation region, (b), (d) crack propagation region.

state at the top of a propagating crack, and initiate the appearance of secondary cracks [18, 19].

The lowest values of impact strength $KCV^{-40} = 144-156$ J/cm² are demonstrated by the specimens of weld joints manufactured by the traditional technology. In the specimen with a notch at the center of an SAW joint, the crack propagates in a straightline fashion (Fig. 3c). The crack nucleation region is limited by the width of 0.5 mm and has a dimple relief (Fig. 6a). The central area of fracture represents a developed surface with numerous secondary cracks. The main crack propagates by the quasi-chipping mechanism, and fracture occurs both over the body of a grain and along the boundaries of grains (Fig. 6b). The groups of facets are joined in the predominant occurrence plane close to the crystallographic plane of chip in body-centered cubic metals of type (100). The size of facets

≈100 μm is comparable with the width of columnar grains formed in the process of weld joint crystallization, and an oval shape of such areas reproduces the cross section of cast grains. Secondary cracks nucleate on the boundaries of grains and propagate to the intersection with the other group of planes (100) with an unfavorable orientation to form thereby the conglomerates of facets in adjacent grains.

Minimal work is spent on the fracture of the specimen with a notch on the welding line of the SAW joint. The crack propagation vector corresponds to the impact direction (Fig. 3d). The nucleation area of the main crack is almost absent. The fracture surface including the region in the immediate proximity to the notch is entirely formed by the mechanism of brittle intercrystallite fracture (Figs. 6c and 6d).

CONCLUSIONS

The comparative analysis of the structure, impact strength, and fracture character of weld joints manufactured in pipes with a diameter of 1420 mm and a wall thickness of 30 mm by hybrid HLAW + SAW and classic double SAW technologies has been performed.

It has been revealed that the phase composition of the remelted metal and heat-affected zone in a weld joint manufactured by HLAW and SAW is identical, but the structure scale essentially differs. The columnar grains in the HLAW joint metal are filled with α-bainite phase crystals and outlined by a ferrite framework, and a completely bainite structure is formed in the heat-affected zone. The width of columnar crystals, as well as the size of a "former" austenite grain in the overheating zone, is 40−60 and 150−200 μm in HLAW and SAW joints, respectively.

It has been established that the specimen of HLAW joints demonstrate an increased level of impact strength, whose appreciable share is the specific crack nucleation work. The structural dispersity inherent in the HLAW joint metal and heat-affected zone is promotive for the tough-ductile mechanism of fracture throughout the entire propagation trajectory of the main crack. A low facture energy consumption inherent to the specimens of weld joints manufactured by the conventional SAW technology is caused by the limited crack nucleation stage and a quasi-brittle character of fracture, whose relief reproduces the coarse-grained structure of the SAW joint metal and heat-affected zone.

FUNDING

REFERENCES

1. L. I. Efron, *Metal Science in "Large" Metallurgy. Pipe Steels* (Metallurgizdat, Moscow, 2012) [in Russian].

2. C. Liu and S. D. Bhole, "Challenges and developments in pipeline weldability and mechanical properties," Sci. Technol. Weld. Joining **18**, No. 2, 169−181 (2013).

3. E. Shigeru and N. Naoki, "Development of thermo-mechanical control process (TMCP) and high performance steel in JFE," JFE Tech. Rep., No. 20, 1−7 (2015).

4. A. N. Bortsov, I. P. Shabalov, A. A. Velichko, K. Yu. Mentyukov, and I. Yu. Utkin, "Features of multi-electrode submerged arc welding in the production of high-strength thick-walled pipes," Metallurg, No. 4, 69−76 (2013).

5. L. A. Efimenko, T. S. Esiev, D. V. Ponomarenko, S. P. Sevast'yanov, and I. Yu. Utkin, "Effect of heat treatment on the impact strength of the metal of welded joints of pipes made by multi-arc submerged arc welding," Metallurg, No. 3, 59−63 (2018).

6. C. Churiaque, M. Chludzinski, M. Porrua-Lara, A. Dominguez-Abecia, F. Abad-Fraga, and J. M. Sánchez-Amaya, "Laser hybrid butt welding of large thickness naval steel," Metals. **9**, No. 1, 100 (2019). https://doi.org/10.3390/met9010100

7. B. Acherjee, "Hybrid laser arc welding: State-of-art review," Opt. Laser Technol. **99**, 60−71 (2018).

8. *The Theory of Laser Materials Processing. Heat and Mass Transfer in Modern Technology*, Ed. by J. Dowden (Springer, Berlin, 2009).

9. A. P. Romantsov, M. A. Fedorov, A. A. Chernyaev, and A. O. Kotlov, RF Patent No. 2640105 (2017).

10. S. E. Gook, A. V. Gumenyuk, and M. Retmaier, "Hybrid laser-arc welding of high-strength API X80 and X120 pipe steels," Global'naya Yadernaya Bezopasnost', No. 1, 21−35 (2017).

11. J. Górka, "Structure and properties of hybrid laser arc welded-joints (laser beam − mag) in thermo-mechanical control processed steel S700mc of 10 mm thickness," Arch. Metall. Mater. **63**, No. 3, 1125−1131 (2018).

12. I. Yu. Utkin, L. A. Efimenko, V. Yu. Bobrinskaya, and O. E. Kapustin, "Evaluation of the role of vanadium and molybdenum in changing the kinetics of austenite decomposition and the mechanical properties of the simulated overheating zone of low-carbon niobium steels," Phys. Met. Metallogr. **122**, No. 7, 718−724 (2018).

13. L. A. Efimenko, O. E. Kapustin, D. A. Ponomarenko, I. Yu. Utkin, M. A. Fedorov, and A. I. Romantsev, "Features of the formation of the structure and properties of welded joints in laser-hybrid welding of longitudinal pipe joints," Metallurg, No. 11, 63−68 (2020).

14. GOST ISO 3183−2015. *Steel Pipes for Pipelines of the Oil and Gas Industry*.

15. STO Gazprom 2-4.1-713-2013. Technical Requirements for Pipes and Fittings.

16. GOST 6996−66. Methods for Determination of Mechanical Properties.

17. Y. Kimura, T. Inoue, F. Yin, and K. Tsuzaki, "Inverse temperature dependence of toughness in an ultrafine grain-structure steel," Science **320**, No. 5879, 1057−1060 (2008).

18. A. S. Dolzhenko, P. D. Dolzhenko, A. N. Belyakov and R. O. Kaibyshev, "Microstructure and impact toughness of high-strength low-alloy steel after tempforming," Phys. Met. Metallogr. **122**, No. 10, 1014−1022 (2021).

19. I. L. Yakovleva, N. A. Tereshchenko, D. A. Mirzaev, A. V. Panov, and D. V. Shaburov, "Impact toughness and plastic properties of composite layered samples as compared to monolithic ones," Phys. Met. Metallogr. **104**, No. 2, 203−211 (2007).

Translated by E. Glushachenkova